LAWRENCE
LIVERMORE
NATIONAL
LABORATORY

UCRL-CONF-227154

Large-eddy simulation of round turbulent jets using the Inertial LES method with multifractal subgrid-scale modeling

G. Burton

January 10, 2007

International Workshop on the Physics of Compressible Turbulent Mixing
Paris, France
July 17, 2006 through July 21, 2006

e-mail: burton29@llnl.gov

Large-eddy simulation of round turbulent jets using the Inertial LES method with multifractal subgrid-scale modeling

Gregory BURTON[1]

[1] *Lawrence Livermore National Laboratory, Livermore, CA 94550 USA*

Abstract: Large-eddy simulation of passive scalar mixing by a fully three-dimensional round incompressible turbulent jet is evaluated using the Inertial LES methodology with multifractal subgrid-scale modeling. The Inertial LES approach involves the direct calculation of the inertial term $\overline{u_i\,u_j}$ in the filtered incompressible Navier-Stokes equation and the scalar flux term $\overline{u_j\,\phi}$ in the filtered advection-diffusion equation, using models for the subgrid velocity field $\mathbf{u}^{sgs}$ and the subgrid scalar-concentration field $\boldsymbol{\phi}^{sgs}$. In this work, the models are based on the multifractal structure of the subgrid enstrophy $2\mathcal{Q}^{sgs}(\mathbf{x},t) \equiv \boldsymbol{\omega}^{sgs}\cdot\boldsymbol{\omega}^{sgs}$ and scalar-dissipation $\boldsymbol{\chi}^{sgs}(\mathbf{x},t) \equiv D\nabla\boldsymbol{\phi}^{sgs}\cdot\nabla\boldsymbol{\phi}^{sgs}$ fields, respectively. No artificial viscosity or diffusivity constructs are applied and no explicit dealiasing is performed. Numerical errors are controlled by the application of an adaptive backscatter limiter. The present work summarizes the initial evaluation of the Inertial LES approach in the context of the round turbulent jet, including examinations of jet self-similarity and the scale-to-scale distribution of kinetic and scalar energy in the jet far field. These inquiries confirm that the Inertial LES method accurately recovers the large scale structure of this complex turbulent shear flow.

1 INTRODUCTION

The free round turbulent jet is perhaps the most extensively studied of the canonical free turbulent shear flows. Turbulent jets are important in a variety of industrial applications, such as fuel injectors, furnaces and rocket engines, as well as in high energy-density phenomena such as astrophysical jets and inertial confinement fusion. The enormous range of length and time scales generated by such flows, however, makes high-resolution laboratory or field study of most of them difficult or impossible. The multiplicity of scales also prevents direct numerical studies (DNS) of such flows, since fully resolving all dynamically-significant scales would require computational power well beyond present-day capabilities. Currently, therefore, the most promising method to study such flows on the computer is through large-eddy simulation (LES), in which only the larger turbulent scales are calculated explicitly, while the smaller, unresolved scales are modeled. However, most presently-available modeling techniques lack the fidelity necessary for LES to become a more widely-accepted tool for scientific and engineering work.

2 INERTIAL LES METHOD

2.1 Multifractal subgrid modeling

Recently, Inertial LES with multifractal subgrid modeling has been proposed as a new, physically-based technique for obtaining high-fidelity large-eddy simulations [1, 2]. In this approach, the filtered Navier-Stokes momentum equation, given by

$$\frac{\partial\,\overline{u}_i}{\partial t} + \frac{\partial}{\partial x_j}\,\overline{u_i\,u_j} - \nu\,\frac{\partial^2\,\overline{u}}{\partial x_j \partial x_j} = 0\,, \tag{2.1}$$

is solved by explicitly calculating the filtered inertial term $\overline{u_i\,u_j}$. Similarly, the filtered advection-diffusion equation, given by

$$\frac{\partial\overline{\phi}}{\partial t} + \frac{\partial}{\partial x_j}\,\overline{u_j\,\phi} - D\frac{\partial^2\overline{\phi}}{\partial x_j \partial x_j} = 0\,, \tag{2.2}$$

is solved by explicitly calculating the filtered scalar-flux term $\overline{u_j\,\phi}$. This approach represents a "return-to-first-principles" in LES methodology, since the unclosed terms in (2.1) and (2.2) are calculated in their original

forms, *i.e.,* as nonlinear stresses, rather than as linear stresses modeled with the gradient-diffusion hypothesis, the approach taken by most current LES methods. The nonlinear terms may be expanded, giving

$$\overline{u_i\,u_j} \equiv \overline{\overline{u}_i\,\overline{u}_j} + \overline{\overline{u}_i\,u_j^{sgs}} + \overline{u_j^{sgs}\,\overline{u}_j} + \overline{u_j^{sgs}\,u_j^{sgs}} \tag{2.3}$$

$$\overline{u_j\,\phi} \equiv \overline{\overline{u}_j\,\overline{\phi}} + \overline{\overline{u}_j\,\phi^{sgs}} + \overline{u_j^{sgs}\,\overline{\phi}} + \overline{u_j^{sgs}\,\phi^{sgs}}\,, \tag{2.4}$$

indicating that the terms involve interactions between resolved and subgrid velocities and scalar fields. Thus, the Inertial LES approach requires models for the subgrid velocities u_j^{sgs} and scalar fluctuations ϕ^{sgs}.

Here, these subgrid models are derived from the multifractal structure present in hydrodynamic turbulence at inertial-range scales. This structure has been confirmed in numerous previous studies [7, 11]. Multifractal structure in the enstrophy field, $2\mathcal{Q}(\mathbf{x},t) \equiv \boldsymbol{\omega}\cdot\boldsymbol{\omega}$, is used first to develop an analytical model for the subgrid vorticity field $\boldsymbol{\omega}^{sgs}(\mathbf{x},t)$. The Biot-Savart law is then employed to relate the analytical model for $\boldsymbol{\omega}^{sgs}(\mathbf{x},t)$ to the subgrid velocity field $u_j^{sgs}(\mathbf{x},t)$. The analytical model for $u_j^{sgs}(\mathbf{x},t)$, in turn, may be simplified to obtain a computationally tractable model for the subgrid velocity field $u_j^{sgs}(\mathbf{x},t)$. A similar approach is taken to derive a model for the subgrid scalar-fluctuation field $\phi^{sgs}(\mathbf{x},t)$ from multifractal structure present in the scalar-dissipation field $\chi(\mathbf{x},t) \equiv D\nabla\boldsymbol{\phi}\cdot\nabla\boldsymbol{\phi}$. Here, the Green's function operator is employed to relate an analytical model for the subgrid scalar-gradient field $\nabla\boldsymbol{\phi}^{sgs}(\mathbf{x},t)$ to the subgrid scalar-fluctuation field $\phi^{sgs}(\mathbf{x},t)$, from which a computational model for $\phi^{sgs}(\mathbf{x},t)$ is derived. In their final forms, both models involve transforming the smallest-resolved scale Δ velocity and scalar fields, as

$$u_j^{sgs}(\mathbf{x},t) \approx \mathcal{B}\,u_j^{\Delta}(\mathbf{x},t) \tag{2.5}$$

$$\phi^{sgs}(\mathbf{x},t) \approx \mathcal{D}\,\phi^{\Delta}(\mathbf{x},t) \tag{2.6}$$

where $\mathcal{B}$ and $\mathcal{D}$ are functions of the number of subgrid scales within an LES grid cell. Detailed development of the subgrid velocity and scalar models are provided in [1] and [3]. Prior evaluation of the Inertial LES method indicates that it reproduces more accurately the local momentum and energy transfer between the resolved and subgrid scales than traditional subgrid modeling approaches [2, 3].

2.2 Backscatter limiting

Numerical errors in the Inertial LES method are controlled here by an adaptive backscatter limiter, a refinement of the technique introduced by Burton & Dahm [2]. That work demonstrated that numerical errors may be effectively controlled by selectively reducing the magnitude of those nonlinear stresses in (2.3) and (2.4) responsible for the reverse transfer of energy from the subgrid to the resolved field during a simulation. To implement such a limiter, the filtered inertial stresses $\overline{u_i\,u_j}$ responsible for backscatter of kinetic energy are first identified as those that satisfy

$$\overline{u_{(i)}\,u_{(j)}}\,S_{(ij)} > 0\,, \tag{2.7}$$

where $2\,S_{ij} \equiv (\partial u_i/\partial x_j + \partial u_j/\partial x_i)$ and where $(\,\cdot\,)$ indicates that no summation is implied. The magnitude of the stress components satisfying (2.7) then are reduced by a factor $C_{\mathcal{B}}$ giving

$$\widehat{\overline{u_i\,u_j}} \equiv C_{\mathcal{B}}\,\overline{u_i\,u_j}\,, \tag{2.8}$$

and the reduced inertial stress is then applied to the momentum update in (2.1). A similar strategy is applied to the passive-scalar equation of (2.2). There, backscatter of scalar energy will occur whenever

$$\overline{u_{(j)}\,\phi}\,\nabla\phi_{(j)} > 0\,. \tag{2.9}$$

Where (2.9) is satisfied, the magnitude of the scalar-flux component is reduced by a factor C_ϕ giving

$$\widehat{\overline{u_j\,\phi}} \equiv C_\phi\,\overline{u_j\,\phi}\,. \tag{2.10}$$

The reduced scalar-flux component is then applied to update the scalar field in (2.2). For both the momentum and the scalar updates, this strategy has the effect of canceling numerical errors arising during the simulation. In the current approach, the values $C_{\mathcal{B}}$ and C_ϕ are determined locally during the simulation.

3 COMPUTATIONAL METHOD

The numerical scheme consists of a standard pressure-correction algorithm on a regular cartesian mesh with primitive variables stored at staggered locations following the method of Harlow & Welch [9]. All spatial derivatives are discretized using 4th-order centered operators, while an explicit 3rd-order Runge-Kutta scheme is used for temporal integration. All simulations employ a resolution of $Nx \times Ny \times Nz \equiv 384 \times 128 \times 128$ points, with $\mathbf{x}$ the downstream direction. Cross stream directions are periodic over the interval $L = 2\pi$. This configuration permits an exact, direct solution of the Poisson equation using standard FFT methods. At the jet outflow, the nonreflective boundary condition of Tang & Grimshaw [13] is implemented. The jet inlet profile consists of a hyperbolic tangent function to which a small co-flow $U_{co} = 0.075\,U_o$ has been added. This has been shown to be a realistic approximation of the actual inlet found in round jets [8]. The inlet width is set at $D \equiv \pi/5$, which in conjunction with the velocity co-flow, has been shown to minimize the impact of the cross-stream periodicity on the downstream development of the jet [5]. All simulations are performed at a relatively high Re_D of $25,000$, which provides for significant unresolved turbulence in the jet's subgrid field.

4 RESULTS

The present work reports only on the initial validation studies of the Inertial LES method in the round turbulent jet configuration, focusing on the fidelity with which the large-scale features of the velocity and scalar fields are reproduced. Figure 1 shows two-dimensional extracts at the jet centerline in the $\mathbf{x}-\mathbf{z}$ plane for the vorticity magnitude field (*top*) and scalar-fluctuation field (*bottom*). These provide a qualitative assessment of the flow field generated by the Inertial LES method. In each frame, zero magnitude is depicted in black while the highest values are depicted in white. The graphics show the characteristic decay of the jet's core by $\sim 5D$ downstream. The angle subtended by the jet expansion cone from the centerline is estimated to be $13.4\,^\circ$, close to the value of $12\,^\circ$ reported by prior studies [6].

As the round turbulent jet is known to develop a scale-similar velocity profile in the far-field region [14], it is useful to examine how well the Inertial LES approach attains and preserves a self-similar state. Figure 2 illustrates four velocity-component profiles as functions of the radial-similarity variable $\boldsymbol{\eta} \equiv r/(x - x_o)$ at five planes, $x/D = [\,17.5,\ 20,\ 22.5,\ 25,\ 27.5,\ 30\,]$, in the far-field region (*clockwise, from upper left*): streamwise mean velocity $U_x(\boldsymbol{\eta})$, streamwise fluctuation velocity $u_x(\boldsymbol{\eta})$; radial fluctuation velocity $u_r(\boldsymbol{\eta})$; and azimuthal fluctuation velocity $u_\theta(\boldsymbol{\eta})$. Each of the depicted distributions shows good collapse at the given downstream planes, indicating that the Inertial LES system reaches and preserves self-similarity, consistent with prior experimental studies [10]. The relatively weaker convergence near the centerline of the jet reflects the smaller number of sampling locations at small $\boldsymbol{\eta}$ and would likely improve over longer simulation times. Figure 3 examines the self-similarity of the scalar concentration field as a function of $\boldsymbol{\eta}$ from statistics gathered at the same five cross-stream planes. Four moments of the scalar concentration field are evaluated (*clockwise, from upper left*): mean scalar concentration $\langle\phi\rangle(\boldsymbol{\eta})$; root-mean-square scalar fluctuations $\phi^{rms}(\boldsymbol{\eta})$; scalar skewness $\mathcal{S}^3(\boldsymbol{\eta})$; scalar flatness $\mathcal{K}^4(\phi)(\boldsymbol{\eta})$. As compared to the velocity field statistics, the radial distributions for the scalar-field statistics show better collapse at $\boldsymbol{\eta}$ values near the jet centerline.

Figure 4 illustrates extracts from timeseries data of the velocity (*top*) and scalar (*bottom*) fields on the jet centerline at $x/D = 27.5$, collected over approximately 1000 timesteps after the jet had reached a statistically-stationary state. Subtle differences can be detected between these timeseries profiles, as the scalar field appears to exhibit the "ramp-cliff" structures that typically characterize scalar fields driven by large-scale anisotropic forcing, like the present shear flow [15]. Figure 5 shows the power spectra for the full velocity and scalar timeseries data sets; (*left*) spectrum of the kinetic energy field vs. time, (*right*) spectrum of the scalar energy field $E_\phi(k)$ vs. time, where $2\,E_\phi = \boldsymbol{\phi}^2(t)$. A $-5/3$ reference slope is provided for comparison. Both figures indicate that the kinetic and scalar energy distributions slightly exceed the $k^{-5/3}$ scaling predicted by Kolmogorov theory [4].

The present investigation confirms that the Inertial LES method accurately recovers the significant large scale structure of both a fully three-dimensional round turbulent jet and the scalar concentration field mixed by it. In the future, the Inertial LES method with multifractal subgrid-scale modeling will be used to study passive-scalar mixing at high Schmidt number ($Sc \gg O(1)$) in a three-dimensional round turbulent jet.

This work was performed under the auspices of the U. S. Department of Energy by University of California, Lawrence Livermore National Laboratory under contract W-7405-Eng-48.

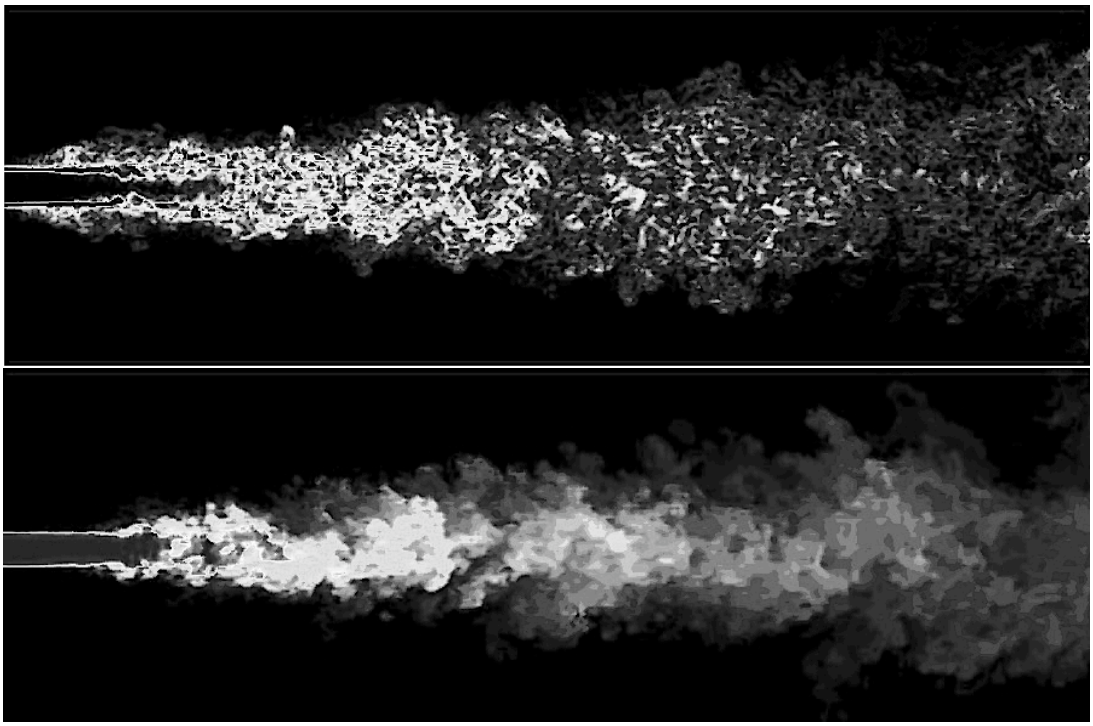

Fig. 4.1. Two-dimensional cross-sections from fully three-dimensional large eddy simulation of round turbulent jet at $Re_D \approx 25,000$ using the Inertial LES method with multifractal subgrid-scale modeling. *(Top)* Vorticity field magnitude with black as $|\omega| \equiv 0$ and white as $|\omega| \equiv 4.32$.*(Bottom)* Scalar fluctuation field with black as $\phi \equiv 0$ and white as $\phi \equiv 1$. From the jet virtual origin, the jet cone of expansion subtends an angle from the centerline of $\theta \approx 13.4^\circ$, close to the estimate of $\theta \approx 12^\circ$ reported in experimental studies by Dowling & Dimotakis [6].

REFERENCES

[1] Burton, G.C. and Dahm, W.J.A. 2005, Multifractal subgrid-scale modeling for large-eddy simulation. I. Model development and *a priori* testing. *Phys. Fluids* **17**, 075111.

[2] Burton, G.C. and Dahm, W.J.A. 2005, Multifractal subgrid-scale modeling for large-eddy simulation. II. Backscatter limiting and *a posteriori* evaluation. *Phys. Fluids* **17**, 075112.

[3] Burton, G.C. 2005, Large-eddy simulation of passive-scalar mixing using multifractal subgrid-scale modeling. *Annual Research Briefs*, Center for Turbulence Research, Stanford, CA

[4] Corrsin, S. 1951, On the spectrum of isotropic temperature fluctuations in isotropic turbulence. *J. Appl. Phys.* **22**, 469.

[5] da Silva, C.B. and Métais, O. 2002, Vortex control of bifurcating jets: A numerical study. *Phys. Fluids* **14**, 3798-3819.

[6] Dowling, D.R. and Dimotakis, P.E., 1990. Similarity of the concentration field of gas-phase turbulent jets. *J. Fluid Mech.* **218** 109-141.

[7] Frederiksen, R.D., Dahm, W.J.A. and Dowling, D.R., 1997, Experimental assessment of fractal scale similarity in turbulent flows. Part 3. Multifractal Scaling. *J. Fluid Mech.***338** 127-155.

[8] Freymuth, P. 1966, On transition in a separated laminar boundary layer. *J. Fluid Mech.* **25**, 683.

[9] Harlow, F.W. and Welch, J.E. 1965, Numerical calculation of time-dependent viscous incompressible flow of fluids with free surface. *Phys. Fluids* **8**, 2182-2189.

[10] Hussein, H.J., Capp, S.P. and George, W.K. 1994, Velocity measurements in a high-Reynolds-number, momentum-conserving, axisymmetric, turbulent jet. *J. Fluid Mech.* **258**, 31-75.

[11] Meneveau, C. and Sreenivasan, K.R. 1991, The multifractal nature of turbulent energy dissipation. *J. Fluid Mech.* **224**, 429-459.

[12] Michalke, A. and Hermann, G. 1982, On the inviscid instability of a circular jet with external flow. *J. Fluid Mech.* **114**, 343.

[13] Tang, Y. and Grimshaw, R. 1996, Radiation Boundary Conditions in Barotropic Coastal Ocean Numerical Models. *J. Comp. Phys.* **123**, 96-110.

[14] Tennekes, H. and Lumley, J.L. 1972, A First Course in Turbulence. *MIT Press*, New York.

[15] Warhaft, Z. 2000, Passive scalars in turbulent flows. *Ann. Rev. Fluid Mech.* **32**, 203-240.

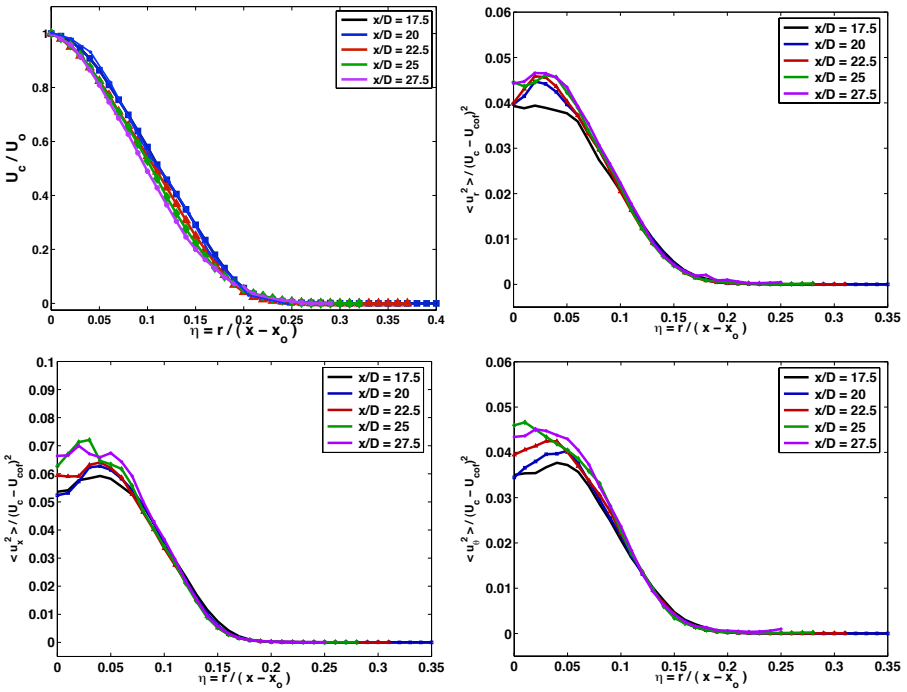

Fig. 4.2. Cross-stream profiles of the first four moments of the velocity fluctuation field vs. similarity variable $\boldsymbol{\eta} \equiv r/(x - x_o)$. Clockwise from upper left: mean streamwise velocity, $\langle u \rangle(\boldsymbol{\eta})$; streamwise fluctuation, $u_x(\boldsymbol{\eta})$; radial velocity fluctuation, $u_r(\boldsymbol{\eta})$; azimuthal velocity fluctuation, $(\boldsymbol{\eta})$. Reasonable collapse of the scaled cross-stream profiles is obtained at the five planes examined in the jet far field, $x/D = [\,17.5,\ 20,\ 22.5,\ 25,\ 27.5,\ 30\,]$.

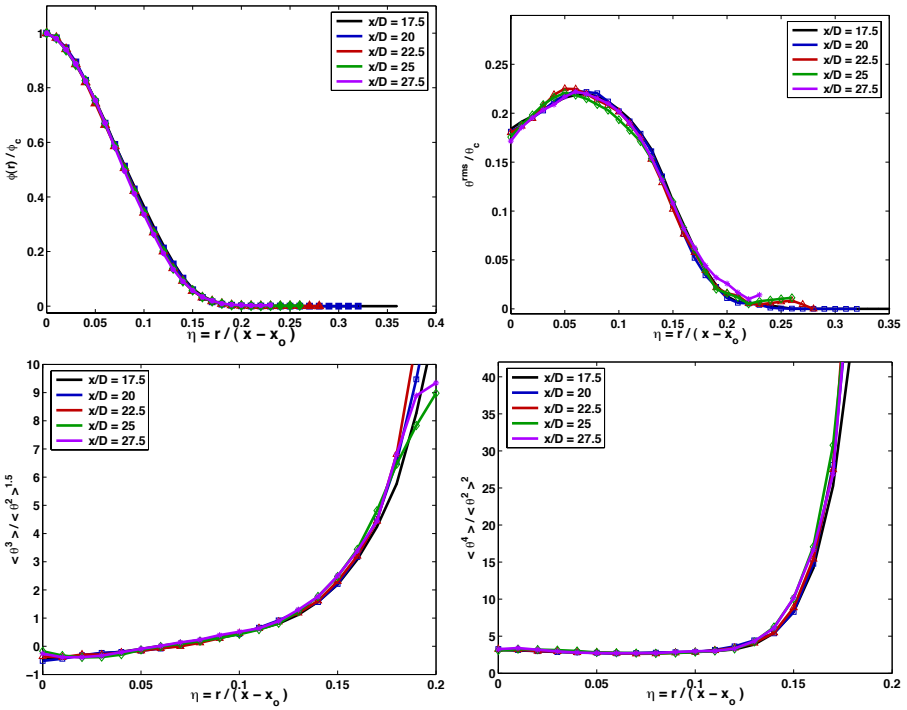

Fig. 4.3. Cross-stream profiles of the first four moments of the scalar concentration field vs. similarity variable $\boldsymbol{\eta} \equiv r/(x - x_o)$. Clockwise from upper left: mean scalar concentration, $\langle \phi \rangle(\boldsymbol{\eta})$; scalar fluctuation r.m.s., $\phi^{'}(\boldsymbol{\eta})$; scalar-fluctuation skewness, $\mathcal{S}^3(\phi^{'})$; and scalar-fluctuation kurtosis, $\mathcal{K}^4(\phi^{'})$.

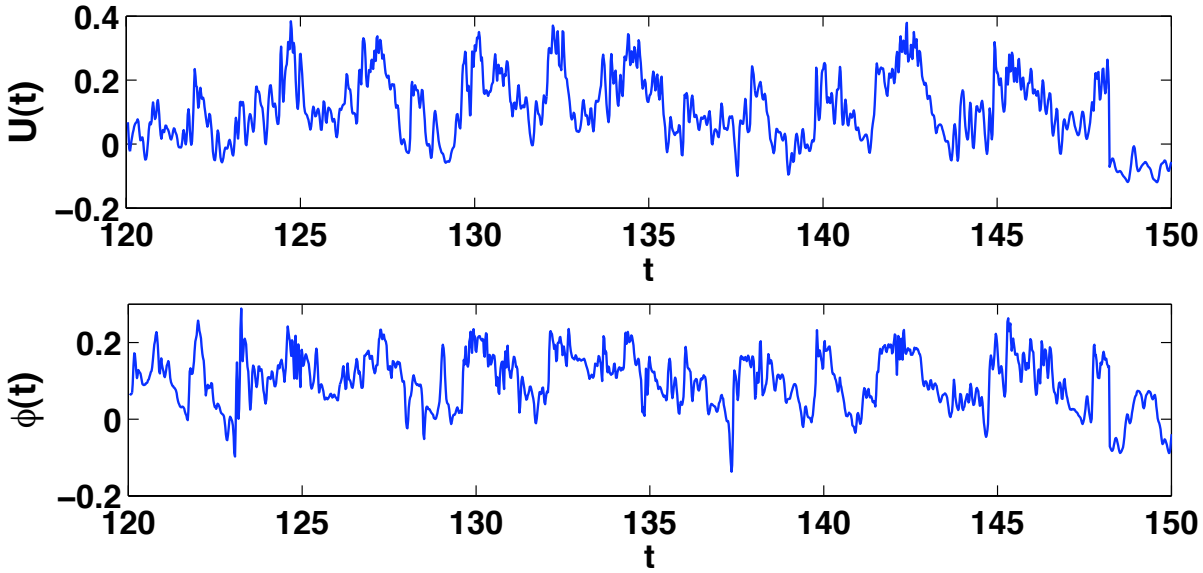

Fig. 4.4. Sample timeseries extracts of the stream-wise velocity field (*top*) and scalar concentration field (*bottom*) from fully three-dimensional large eddy simulation of round turbulent jet at $Re_D \approx 25,000$ using the Inertial LES method with multifractal subgrid-scale modeling. Illustrated timeseries were gathered at the jet centerline at the downstream plane $x/D = 27.5$. Note appearance of subtle "ramp-cliff" structures in the scalar timeseries, indicating large scale anisotropic forcing of the scalar field, as discussed in [15].

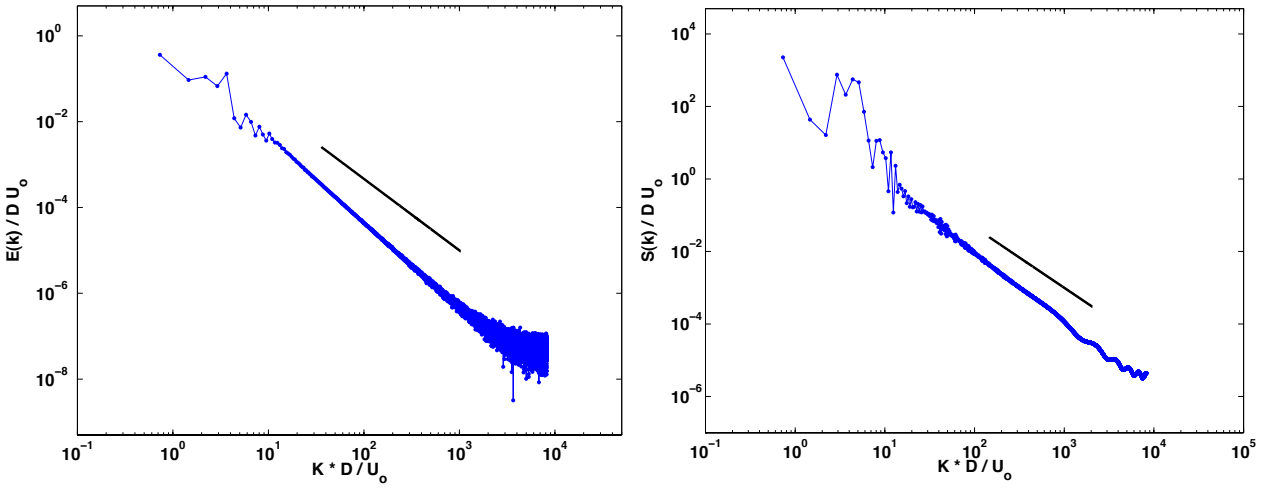

Fig. 4.5. Spectra from timeseries of the stream-wise velocity field (*left*) and scalar concentration field (*right*) from fully three-dimensional large eddy simulation of round turbulent jet at $Re_D \approx 25,000$ using the Inertial LES method with multifractal subgrid-scale modeling. Solid line in each frame provides a $-5/3$ slope for comparison, indicating that both spectra slightly exceed the value predicted by Kolmogorov theory [4].